the plant journal

SOCIETY FOR EXPERIMENTAL BIOLOGY

The Plant Journal (2008) **55**, 1–13 doi: 10.1111/j.1365-313X.2008.03471.x

Changing transcriptional initiation sites and alternative 5′- and 3′-splice site selection of the first intron deploys Arabidopsis PROTEIN ISOASPARTYL METHYLTRANSFERASE2 variants to different subcellular compartments

Randy D. Dinkins[1,†], Susmita Maitra Majee[2,†,‡], Nihar R. Nayak[2,†], David Martin[2,‡], Qilong Xu[2,§,¶], Marisa P. Belcastro[3,††], Robert L. Houtz[2,§], Carol M. Beach[4] and A. Bruce Downie[2,*,‡,§]

[1]*USDA-ARS Forage-Animal Production Research Unit, N220C Agriculture Science Center, North, University of Kentucky, Lexington, KY 40546-0091, USA,*

[2]*Department of Horticulture, University of Kentucky, Lexington, KY 40546-0312, USA,*

[3]*University of Kentucky Agricultural Biotechnology Undergraduate Program, University of Kentucky, Lexington, KY 40546-0312, USA, and*

[4]*Department of Molecular and Cellular Biochemistry, University of Kentucky, Lexington, KY 40546-0509, USA*

Received 4 December 2007; revised 31 January 2008; accepted 6 February 2008; published online 1 May 2008.

*For correspondence (fax +859 257 7874; e-mail adownie@uky.edu).

†These authors contributed equally to this work.

‡University of Kentucky Seed Biology Program.

§University of Kentucky Plant Physiology/Biochemistry/Molecular Biology Program.

¶Present address: Department of Pathobiological Sciences, School of Veterinary Medicine, Louisiana State University, Skip Bertman Drive, Baton Rouge, LA 70803, USA.

††Present address: University of Kentucky Medical School, 800 Rose Street, Lexington, KY 40536, USA.

Summary

Arabidopsis thaliana **(L.) Heynh. possesses two *PROTEIN-L-ISOASPARTATE METHYLTRANSFERASE* (*PIMT*) genes encoding enzymes (EC 2.1.1.77) capable of converting uncoded L-isoaspartyl residues, arising spontaneously at L-asparaginyl and L-aspartyl sites in proteins, to L-aspartate. *PIMT2* produces at least eight transcripts by using four transcriptional initiation sites (TIS; resulting in three different initiating methionines) and both 5′- and 3′-alternative splice site selection of the first intron. The transcripts produce mature proteins capable of converting L-isoaspartate to L-aspartate in small peptide substrates. PIMT:GFP fusion proteins generated a detectable signal in the nucleus. However, whether the protein was also detectable in the cytoplasm, endo-membrane system, chloroplasts, and/or mitochondria, depended on the transcript from which it was produced. On-blot-methylation of proteins, prior to the completion of germination, indicated that cruciferin subunits contain isoaspartate. The implications of using transcriptional mechanisms to expand a single gene's repertoire to protein variants capable of entry into the cell's various compartments are discussed in light of PIMT's presumed role in repairing the proteome.**

Keywords: transcription, splicing, isoaspartate, methyltransferase, subcellular compartment, repair.

Introduction

The proteome is subject to deleterious alteration over time. Because it is more parsimonious to repair damaged protein than to synthesize replacements *de novo*, a rationale explaining the existence of a variety of systems to repair a plethora of protein damage has been established (Hoshi and Heinemann, 2001; Pliyev and Gurvits, 1999; Romero *et al.*, 2004; Schumacher *et al.*, 1996). One repair process involves PROTEIN-L-ISOASPARTATE METHYLTRANSFERASE (PIMT; EC 2.1.1.77) converting isoaspartyl (isoAsp) residues, formed spontaneously from L-aspartate or L-asparagine, back into L-aspartate, usually recovering some or all of the substrate protein's function/catalytic capacity (Figure 1a; Lowenson and Clarke, 1992; Aswad *et al.*, 2000). PROTEIN-L-ISOASPARTATE METHYLTRANSFERASE activity is vitally

© 2008 The Authors
Journal compilation © 2008 Blackwell Publishing Ltd

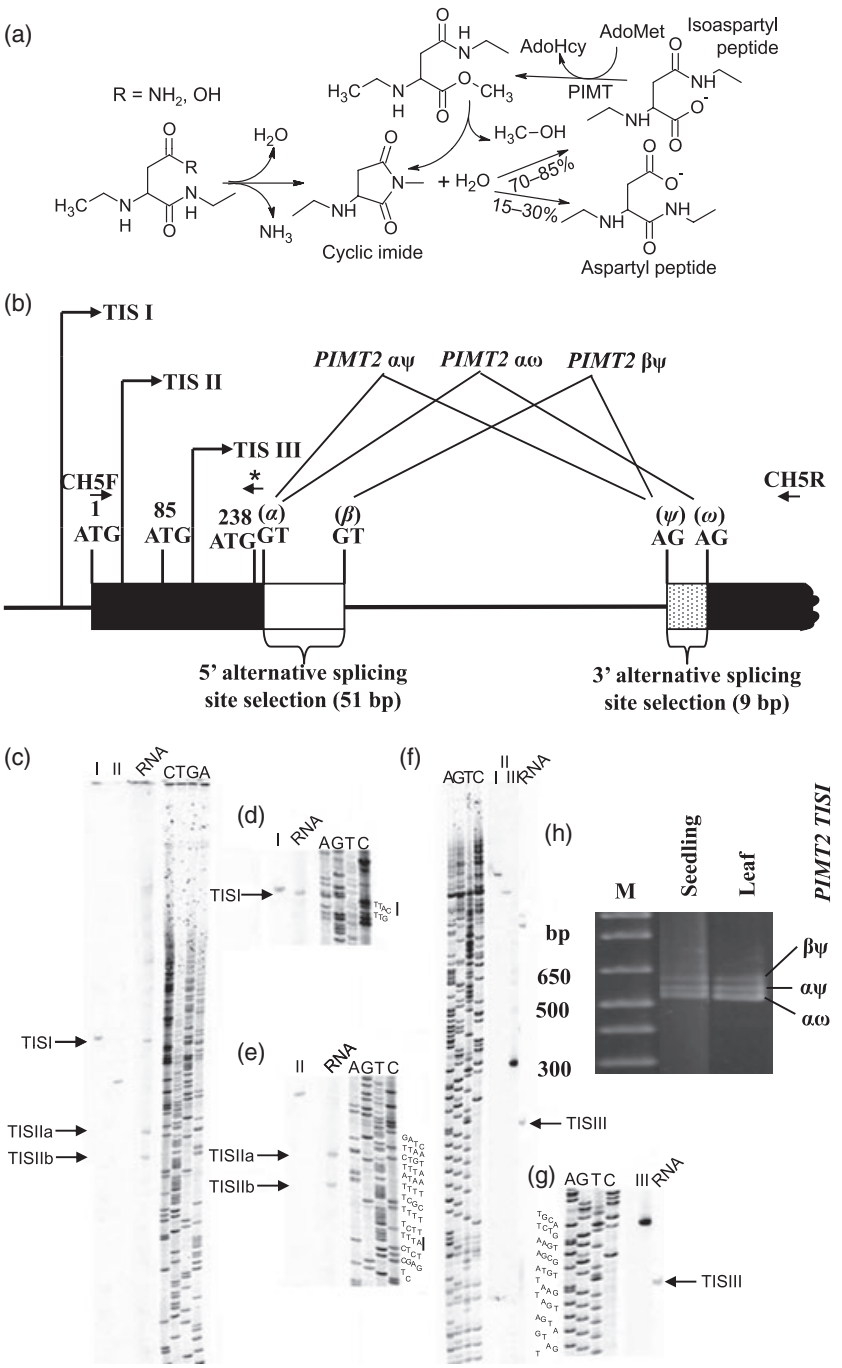

Figure 1. The *PROTEIN ISOASPARTYL METHYLTRANSFERASE2* (*PIMT2*) gene exhibits a complex transcriptional control involving different transcriptional initiation sites (TIS) and 5′- and 3′-alternative splice site selection of the first intron.
(a) Conversion of aspartyl and asparaginyl residues to an unstable succinimide intermediate that can form an aspartyl (15–30% frequency) or an isoaspartyl residue (85–70% frequency). PROTEIN-L-ISOASPARTATE METHYLTRANSFERASE (PIMT) recognizes the isoaspartyl residue, methylates the α-carboxyl forming the side-chain, destabilizing it and re-forming the succinimide residue though the loss of methanol. Iterative cycles of methylation and succinimide formation eventually lead to conversion of most of the isoaspartate to aspartate.
(b) Different TIS regions [determined by 5′-rapid amplification of cDNA ends (5′-RACE)] result in three different, in-frame, initiation codons and 5′ untranslated region lengths. Alternative 5′ splice site selection of the first intron includes (β) or excludes (α) 51 in-frame nucleotides (17 amino acids) in the coding region. Additionally, the 3′ splice site for this intron varies to include (ψ) or exclude (ω) a nine-nucleotide (three-amino-acid) fragment in the coding region. Arrows labeled CH5F and CH5R depict PCR primers spanning the first intron while the arrow (under the asterisk) just 5′ to the first intron was used for both primer extension and sequencing reactions. Primer extension analysis of Arabidopsis RNA verified at least four prominent TISs for *PIMT2*.
(c–g) Control cDNAs were made corresponding to the three TISs identified by 5′-RACE and included in the primer extension reactions as positive controls. These were run in lanes labeled I, II, and III and should be compared with signal from primer extension of leaf RNA (experimental lane labeled RNA in the figures). The TIS identified by primer extension are labeled on the side of the gel with the appropriate designation and an arrow to the left of the band in the RNA lanes.
(h) Only three of four possible splicing variants were amplified from the *PIMT2 TIS I* transcript. Reverse transcriptase-PCR of DNaseI-treated total RNA from seeds (not shown), seedlings, or rosette leaves using primers spanning the first intron. The 5′-most primer (CH5F) specifically bound only cDNA from *PIMT2* transcripts commencing from *TIS I* (Figure 1b). Three bands are discernible in the 4% (w/v) Metaphor agarose gel stained post-run with SYBR-Gold corresponding to βψ, αψ, and αω splice variants.

important in those organisms employing it (David *et al.*, 1999; Kagan *et al.*, 1997; Kim *et al.*, 1997; Visick *et al.*, 1998; Yamamoto *et al.*, 1998). Most Asn or Asp residues in any protein, regardless of subcellular location, are subject to conversion to the abnormal isoAsp. In Arabidopsis, two different *PIMT*s produce proteins found in either the cytoplasm and nucleus (PIMT1; Xu *et al.*, 2004) or nucleus (PIMT2; Xu *et al.*, 2004). A more intense scrutiny of the Arabidopsis *PIMT2* sequence has revealed three additional transcriptional initiation sites (*TIS IIa,b* and *TIS III*) producing shorter transcripts (Villa *et al.*, 2006), two of which result in different initiating methionines commencing proteins that lack the canonical nuclear localization signal (Xu *et al.*, 2004). The transcripts produced from *TIS I*, *II* and *III* can also undergo alternative 5′- as well as 3′-splice site selection of the first intron. We investigated the veracity and consequences of this complex transcriptional and processing phenomenon for protein subcellular localization, reasoning

© 2008 The Authors

that the different transcripts produced proteins capable of deploying throughout the cell to safeguard the intracellular proteome.

Results

Identification of the multiple transcriptional initiation sites of the PIMT2 *gene*

Characterization of *PIMT2* (*At5g50240*) identified 13 5′-rapid amplification of cDNA ends (RACE; specific for capped RNA) products. Two cDNA clones of *PIMT2 TISI*, differing by a nine-nucleotide, 3′-alternative splicing event were assembled and reported (Xu *et al.*, 2004; Figure 1b). Of the remaining 5′-RACE products seven terminated in a region designated as the second transcriptional initiation site (TISII; Figure 1b) and four 5′-RACE amplicons terminated in a region containing a third transcriptional initiation site (TISIII; Figure 1b).

A transcript commencing at TISI was confirmed from amplicons retrieved while verifying 5′- and 3′-alternative splicing variants (see below and Xu *et al.*, 2004) using PCR primers, one of which (CH5F; Figure 1b) bound to the 5′ region of cDNAs synthesized exclusively from TISI transcripts. However, whether the other TISs discovered by 5′-RACE were real or were from truncated mRNA that avoided the dephosphorylation step associated with the capped RNA 5′-RACE protocol (GeneRacer kit, Invitrogen Corp., http://www.invitrogen.com/) remained unresolved.

The riboprobe used to map the 5′-termini of *PIMT2* transcripts by ribonuclease protection assays (RPAs) was prone to self-protection, and so primer extension analysis on total RNA from seedlings or rosette leaves was used instead. For each of the amplicons associated with each TIS, no one consensus nucleotide was consistently identified by RACE as the initiation site. Rather, RACE identified different 5′-termini for each TIS, all within a region of 5–20 bp, depending on the TIS. So, we also wanted to determine whether there were predominant nucleotides from which transcription usually commenced in each TIS region or whether transcription initiation along the *PIMT2* gene was promiscuous. To do this we chose the longest 5′-RACE product discovered for each of the three TISs and amplified *PIMT2* cDNA from it using PCR. These amplicons were diluted and included as positive controls in the primer extension analysis. Primer extension revealed that there were at least four discrete, predominant TISs for *PIMT2* (Figure 1c–g). The TIS I identified by RACE was very similar to that revealed by primer extension (Figure 1c,d), lying between 20 and 23 nucleotides 5′ of the ATG.

The longest TISII discerned using 5′-RACE was considerably longer than two predominant TISIIs discovered by primer extension (Figure 1c,e). Because both of these TISII sites were still 5′ to the translational initiation codon, they were designated TISIIa and TISIIb because they would result in the same protein (Figure 1c,e; labeled TIS Ia and -b (arrows) to the left of the bands in the experimental lanes (RNA)). The difference among the TISII discovered by primer extension (Figure 1e) and that from 5′-RACE was approximately 36 (a) and 48 (b) nucleotides, with TISIIb at least 18 nucleotides 5′ to the ATG.

The TISIII documented by 5′-RACE ('III' over the third lane) was also considerably longer than the most predominant TISIII observed using primer extension (Figure 1f,g labeled TISIII (arrow) in the experimental lanes, RNA). The difference in length was approximately 21 nucleotides (see Figure 1g), which was still 5′ to the translational initiation for the PIMT2 TISIII protein which could not be resolved with the primer used for the primer extension and sequencing (see Figure 1b).

Alternative 5′- and 3′-splice site selection of the first intron

Based on the sequences retrieved from 5′-RACE, *PIMT2* transcripts are subject to alternative 5′- and 3′-splice site selection of the first intron (Figure 1b). At least one amplicon terminating in each of the three transcriptional initiation regions was differentially spliced at the 3′ end. One of seven 5′-RACE products terminating in the TISII region utilized the 5′ alternative splice site (β). Using primers spanning intron I, the 5′-most of which (CH5F) was specific for cDNAs from transcripts commencing at TISI, three amplicons were obtained (Figure 1h) that, when sequenced, corresponded to *PIMT2 TISI*$\beta\psi$, $\alpha\psi$,and $\alpha\omega$. We did not observe amplicons corresponding to a $\beta\omega$ splicing event. Neither did we have indications that the other two introns in *PIMT2* were differentially spliced. We were unable to establish the existence of *PIMT2 TISIII*$\beta\psi$ using 5′-RACE but neither can we exclude this possibility and, based on the presence of a $\beta\psi$ splicing event for the other TIS, determined its existence was probable. Our data indicate that there are no fewer than four predominant transcriptional initiation sites in *PIMT2* (I, IIa, IIb, and III, Figure 2) and that these transcripts can be further modified using either 5′- or 3′-alternative splice site selection of the first intron (Figure 2).

Attempts to verify the existence of proteins translated from the various transcripts *in vivo* were only partially successful due to the attenuation of signal from PIMT2 antibodies during double affinity purification (see Experimental procedures; Xu *et al.*, 2004) to avoid cross-hybridization with PIMT1 (Figure 3a). Nevertheless, a second immunoreactive protein, possibly corresponding to protein from a *PIMT2 TISII* splicing variant, was present in cell fractions containing PIMT2 TISI protein (Xu *et al.*, 2004).

To maximize the sensitivity of the western blot analysis we used antibodies that had undergone a single affinity purification that bound to PIMT1, PIMT2 TISI, TISII, and TISIII (see Experimental procedures). Regardless of where else the PIMT2 proteins resided they were all discernible to some

© 2008 The Authors

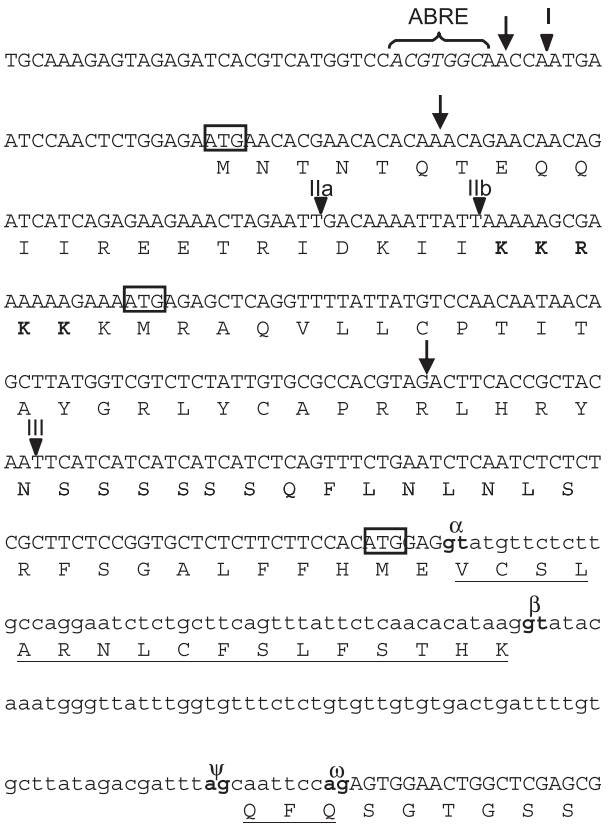

Figure 2. Transcripts from PIMT2 result in a variety of different proteins depending on transcriptional initiation sites (TIS) and splicing.
Regardless of whether transcripts are produced from the longest (downward arrows) or predominant (arrow heads labeled I, IIa, IIb, and III) TIS, they are all associated with a specific translational initiation codon (boxed ATGs). If the most proximal translational initiation codon is used for each TIS, and the same splice variant is examined, the TISI transcripts produce proteins that are 28 amino acids longer than those of TISII and 79 amino acids longer than TISIII. TISII proteins are 51 amino acids longer than TISIII. The TISI protein includes a nuclear localization signal while TISII and TISIII preclude these amino acids. Alternative splicing of the first intron can lengthen the protein by 17 amino acids (using the β rather than the α splice site, underlined) and/or by three amino acids (using the ψ rather than the ω splice site, underlined). The *PIMT2* promoter has many elements related to ABA or stress, including an ABA-response element (ABRE) consensus sequence.

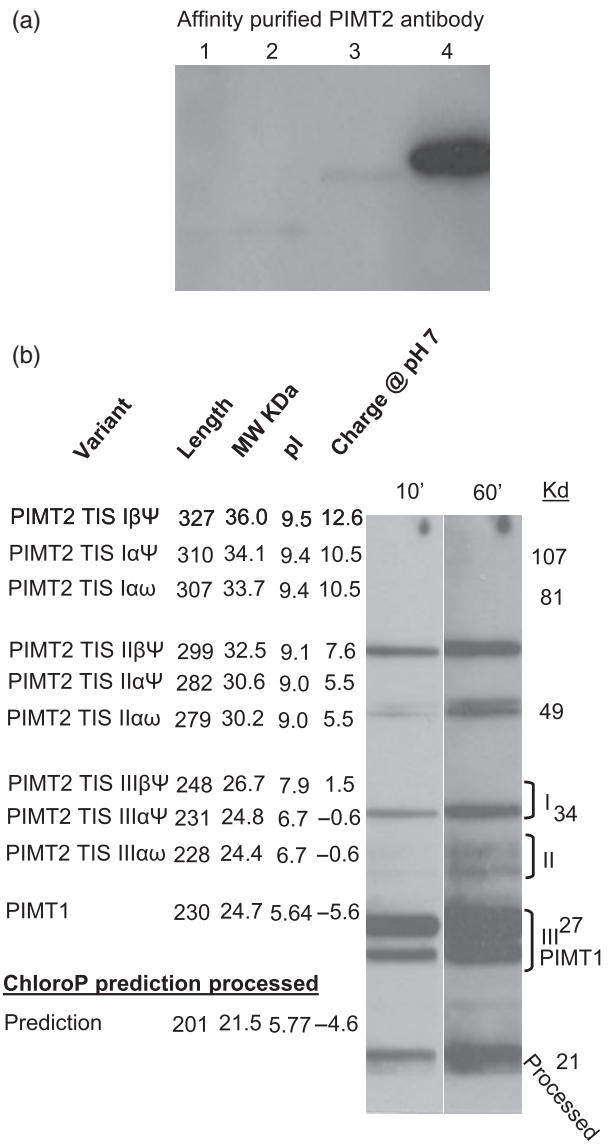

Figure 3. Proteins corresponding to various transcripts are detectable on western blot.
(a) Double affinity purification (see Experimental procedures) used to create a PIMT2-specific-antibody, while eliminating recognition of PIMT1 (Xu *et al.*, 2004) also decreased its capacity to recognizing PIMT2 TISII and PIMT2 TISIII. In all cases 300 ng of recombinant protein was loaded per lane and resolved using 10% acrylamide gel containing SDS. Protein was blotted to membrane and probed with double affinity-purified PIMT2 antibody. Lane 1, PIMT1, lane 2, PIMT2 TISIIIαω; lane 3, PIMT2 TISIIαω; lane 4, PIMT2 TISIαω.
(b) Antibody affinity purified to detect PIMT1 and all PIMT2 variants (see Experimental procedures) was employed to examine Protein-L-isoaspartate methyltransferase (PIMT) protein *in vivo*. Bands in excess of 45 kDa are not attributable to PIMT based on our data. Exposure times (in min) are provided above each lane.

degree in the nucleus (see below) and we reasoned that these forms would retain their N-termini which (barring post-translational modifications) would allow the prediction of immunoreactive band sizes on a western blot. As was the case in a previous study (Xu *et al.*, 2004), we found no indication of a PIMT2 TISIβψ protein (Figure 3b). However, a band corresponding in size to PIMT2 TISIαψ and/or αω was discernible (34.1 and 33.7 kDa, respectively; Figure 3b). Longer exposure of the blot revealed bands that are in the correct size range for all three PIMT2 TIS II proteins generated from the three splicing variants βψ, αψ, and αω (32.5–30.2 kDa; Figure 3b). There are also bands that could correspond to any of the PIMT2 TISIII proteins, including TISIIIβψ (26.7–24.4 kDa; Figure 3b). Because the isoelectric points do not vary between the αψ and αω splice variants, western blots from two-dimensional (2D) gels (data not shown) were no more helpful in determining the exact number of PIMT2 proteins *in vivo* than the one-dimensional

© 2008 The Authors

(1D) blot portrayed (Figure 3b). It is possible that the various proteins produced from the *PIMT2* transcripts include target peptides that are removed upon import into the mitochondria and/or plastids. Predictions of the size of the protein produced upon such import (Figure 3b) corresponded with bands present on the western blot (Figure 3b 'processed') despite the fact that the protein came from crude nuclear preparations.

Subcellular localization of the various PIMT2 proteins in transient assays

Protein subcellular localization was correlated throughout the study with a variety of control fusion proteins targeted to the nucleus (Dinkins *et al.*, 2003b), the mitochondria (Michalecka *et al.*, 2003), the endoplasmic reticulum (ER; Haseloff *et al.*, 1997; Chakrabarty *et al.*, 2007), the cytoplasm and nucleus (Xu *et al.*, 2004), or associated with the microtubules (Smertenko *et al.*, 2004). PIMT2 fused to the green fluorescent protein (GFP; experimental) and appropriate control plasmids using red fluorescent protein (RFP) or DsRED targeted to various subcellular compartments were co-bombarded into cells on gold particles. When expressed alone, without a fusion, the distribution of GFP/RFP and DsRED were very similar, being distributed throughout the cytoplasm and nucleus (Talcott and Moore, 1999; Figure 4a,b). They were not associated with the mitochondria (data not shown) or the chloroplasts (chlorophyll autofluorescence; Figure 4c,d). PIMT1 showed a similar distribution to that of the GFP/RFP/DsRED (Figure 4e) but with a greater propensity to aggregate in threads throughout the cell, surrounding but not entering the chloroplasts (Figure 4e,h). Suspecting that these threads might be cytoskeletal in nature, the distribution of MAP65-1:DsRED and PIMT1 was examined in co-bombarded cells (Figs. 4e–h). There does not seem to be an exact match between where PIMT1 and tubulin are situated but there is some overlap (Figure 4h).

Regardless of transcriptional initiation site or splicing variant, the PIMT2 proteins were all observed in the nucleus in most cells. However, in many instances, the presence of the fusion protein in the nucleus appeared at low levels, probably due to lack of exclusion from the nucleus as seen with GFP alone, and not due to import or sequestering. Indeed, although the nuclear localization signal was only present in PIMT2 proteins translated from a message commencing from the first TIS, none of these proteins had the nucleus as their primary residence (Figure 5; TISI). Instead, both PIMT2 TISI$\alpha\psi$ and PIMT2 TISI$\alpha\omega$ were predominately present in the chloroplasts and in small, motile bodies suspected of being mitochondria (Figure 5 TISI$\alpha\psi$ and $\alpha\omega$). PIMT2 TISI$\beta\psi$ was not observed in the chloroplasts but was present in small motile bodies (Figure 5, $\beta\psi$). Mitochondrial localization was confirmed when cells were co-bombarded with a mitochondrial-targeted RFP construct (Figure 6a–c; Figure S1).

The TISII$\alpha\psi$ and $\alpha\omega$ proteins were prominent in the nucleus to which the AtZFP-DsRED fusion was directed (Figure 5, TISII$\alpha\psi$ and $\alpha\omega$; data not shown). They were also

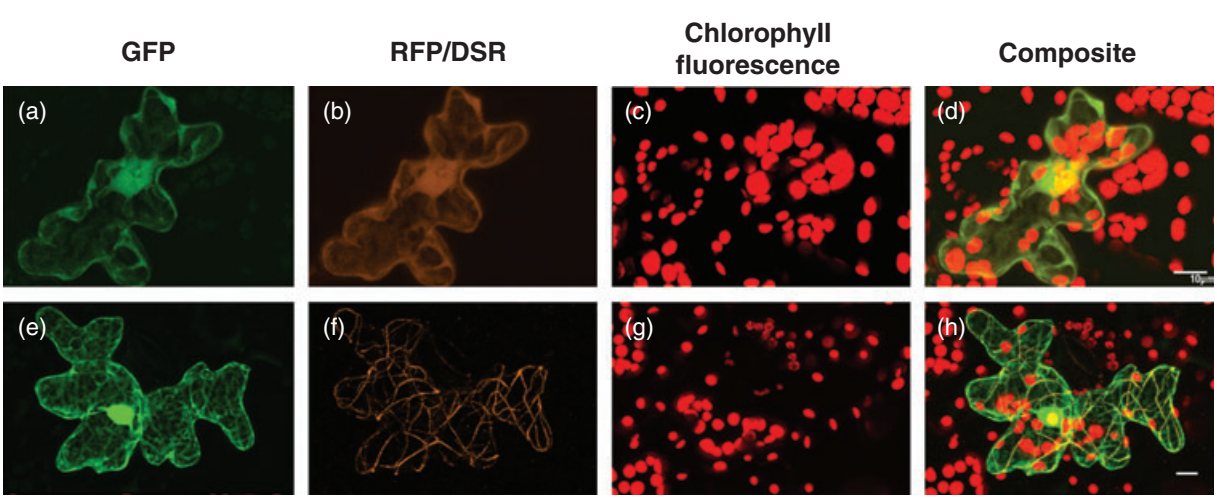

Figure 4. A variety of fusions with fluorescent proteins permitted identification of different subcellular compartments.
(a) GFP alone.
(b) DsRED alone.
(c) Chlorophyll autofluorescence.
(d) Overlay.
(e) PIMT1:GFP.
(f) *Arabidopsis thaliana* microtubule-associated protein 65-1:DsRED.
(g) Chlorophyll autofluorescence.
(h) Overlay. All bars represent 10 μm.

© 2008 The Authors

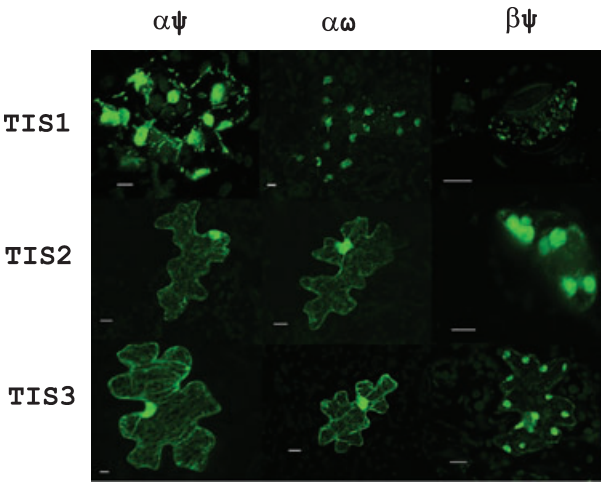

Figure 5. PIMT2 protein variants are dispersed throughout the cell.
PIMT2 TISIαψ and PIMT2 TISIαω were predominately present in the plastids while PIMT2 TISIβψ was present in the mitochondria. Protein translated from *PIMT2 TISII*αψ and *PIMT2 TISII*αω was present in the nucleus and cytoplasm while PIMT2 TISIIβψ protein was predominately present in the chloroplasts and mitochondria. PIMT2 TISIIIαψ, and PIMT2 TISIIIαω were present throughout the cytoplasm and were also in the nucleus. In the cytoplasm they formed pervasive strands. PIMT2 TISIIIβψ protein was predominately in the chloroplasts but some was also associated with or present in the endoplasmic reticulum. All bars represent 5 μm.

present throughout the cell similar to GFP alone (Figure 4a). Both proteins appeared to surround, but not enter, the plastids in the same manner as PIMT1 (data not shown). PIMT2 TISII protein produced from transcript using the β-5′-alternative splice site were present in the chloroplasts and in the mitochondria to which the mitochondrial targeted RFP fusion protein was also directed (Figure 5 TISIIβψ, Figure 6d–f, Figure S2).

There were no differences in subcellular residence of PIMT2 TISIII proteins from transcripts using αψ or αω splice sites, both being located in the nucleus and throughout the cytoplasm (Figure 5, TISIIIαψ and αω). The pervasive strands formed by the GFP-fused PIMT2 TISIII proteins produced from transcript spliced α suggested they might be associated with components of the cytoskeleton. A co-bombarded *MAP65-1* coding region fused to the *DsRED* cDNA indicated that at least some TISIIIαψ and TISIIIαω, like the PIMT1 protein, was co-localized with the MAP65 protein in association with microtubules (Figure 6g–i,j–l; optical sections in Figure S3).

In addition to low-level expression in the nucleus, PIMT2 TISIIIβψ was present in the chloroplasts and was associated with cytoplasmic strands that co-localized with an ER-targeted RFP fusion protein (Figure 5, TISIIIβψ, and Figure 6m–o; FigureS4). The predominant predicted and observed subcellular locale of each PIMT2 isoform were frequently different (Table S1).

Two-dimensional gel electrophoresis, on-blot methylation, matrix assisted laser desorption ionization (MALDI)-time of flight (TOF)-TOF

Attempts to use recombinant Arabidopsis PIMT1 for on-blot methylation (OBM) were unsuccessful while signal from recombinant human PIMT (rHsPIMT) was detectable (Figure 7a) and resolution improved using Enhance spray and X-ray film rather than a tritium screen (Figure 7b). Preparing the blotted extracts for OBM allowed rHsPIMT to renature sufficiently to bind *S*-adenosyl-L-methionine (AdoMet) (Figure 7b). Liquid assays with only rHsPIMT as both enzyme and substrate indicated that the signal was not due to self-repair (data not shown; Lindquist and McFadden, 1994). Seed extracts exhibited several prominent bands (Figure 7b).

Protein abundance based on Coomassie staining did not invariably correspond with signal intensity from OBM (Zhu *et al.*, 2006; Figure 7c). In all, 32 cored samples were sequenced, 27 of which were unique. Five samples (2, 7, 13, 15, 16; Figure 7c) from a separate OBM experiment were cored from their Coomassie-stained gel and these were identified as the same acid/basic subunit from the same gene product (Table S2) demonstrating repeatability.

Discussion

The occurrence of isoaspartate can reduce the catalytic competency of enzymes and otherwise interfere with protein function (Clarke, 2003), although exceptions exist (Curnis *et al.*, 2006; Reissnera and Aswad, 2003). While most Asp- and/or Asn-containing proteins are susceptible to isoaspartate formation to varying degrees (Brennan and Clarke, 1993; Xie and Schowen, 1999), to compensate PIMT is capable of methylating a wide variety of isoaspartyl-containing proteins, albeit with considerable differences in K_m (Lowenson and Clarke, 1991). Therefore, PIMT has the capacity to maintain a functional proteome so long as it has access to it. However, this presents a quandary in many eukaryotes where there is a single *PIMT* gene but multiple protein-containing subcellular compartments, some of which exclude PIMT (O'Connor, 2006). The proteome in subcellular compartments must have other means of removing isoaspartyl-containing proteins, including proteolysis (Bruneau *et al.*, 2006; Tarcsa *et al.*, 2000), tolerance (Najbauer *et al.*, 1996; O'Connor, 1987), or transport into the cytoplasm, whereas elimination of PIMT activity altogether curtails life expectancy, at least in some organisms (Kim *et al.*, 1997).

The most prevalent subcellular target observed in the PIMT2:GFP fusion TISI and TISII isoforms was the chloroplast, except the PIMT TISIβψ isoform, which was targeted specifically to the mitochondria and not observed in the chloroplasts. Overall GFP expression levels were not very

© 2008 The Authors

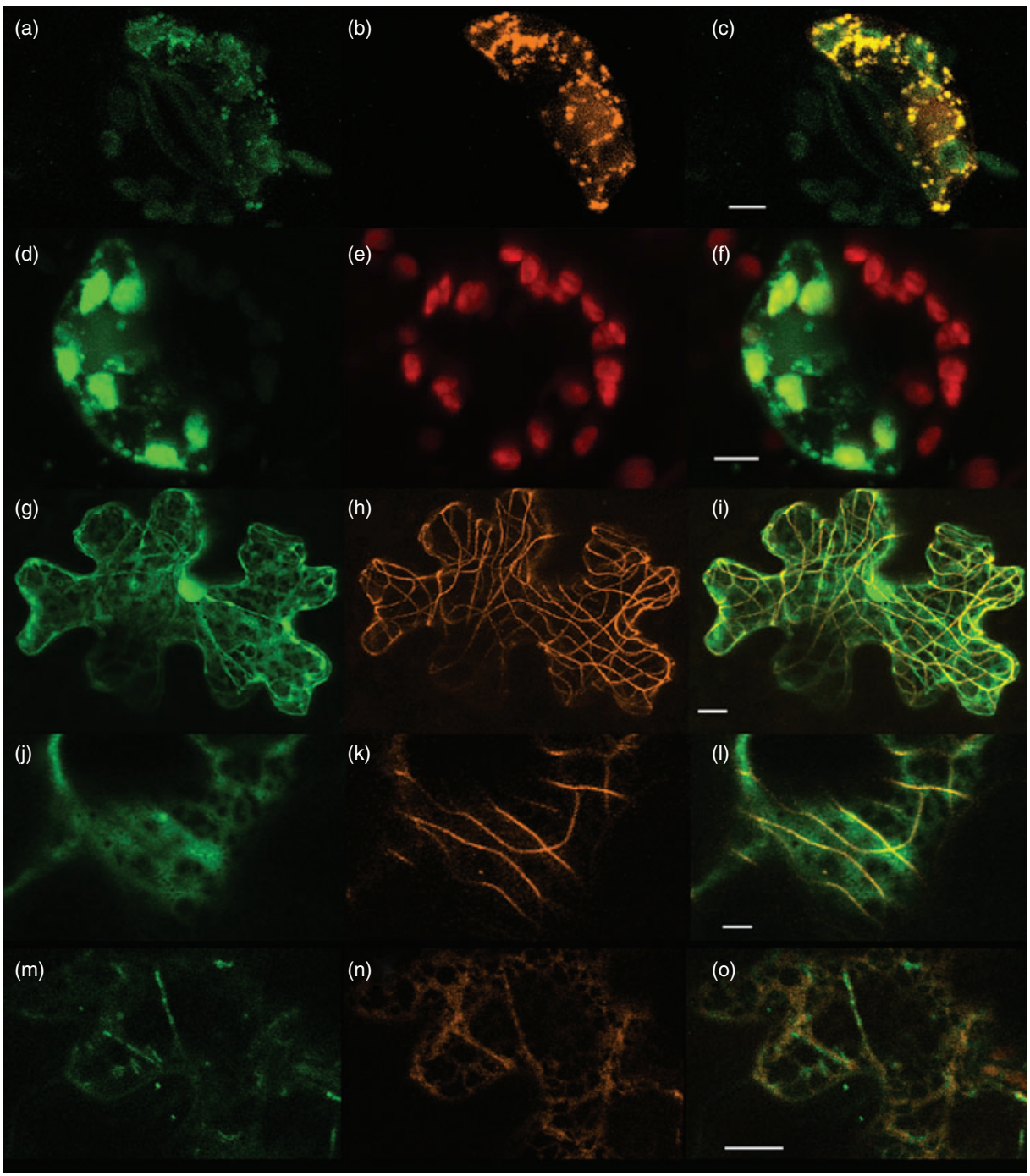

Figure 6. Several PIMT2 proteins can be localized in more than one subcellular compartment.
(a–c) The PIMT2 TISIβψ is prominent in mitochondria although it is also in the nucleus: (a) PIMT2 TISIβψ:GFP; (b) NDA2:RFP; (c) overlay. The bar in the last frame represents 5 μm.
(d–f) The plastidal and mitochondrial distribution of PIMT2 TISIIβψ in the cell: (d) PIMT2 TISIIβψ:GFP; (e) chlorophyll autofluorescence; (f) overlay. The bar in the last frame represents 5 μm.
(g–i) In addition to its presence in the cytoplasm, PIMT2 TISIIIαω:GFP and MAP65-1:DsRED are occasionally associated with each other, co-localizing with tubulin microtubules: (g) PIMT2 TISIIIαω:GFP; (h) MAP65-1:DsRED; (i) overlay. The bar in the last frame represents 10 μm.
(j–l) A close-up of co-localized PIMT2 TISIIIαω:GFP and MAP65-1:DsRED: (j) PIMT2 TISIIIαω:GFP; (k) MAP65-1:DsRED; (l) overlay. The bar in the last frame represents 5 μm.
(m–o) PIMT2 TISIIIßψ; depicting the association of some of this PIMT2 protein and the ER and its presence in the cytoplasm: (m) PIMT2 TISIIIßψ:GFP; (n) ER-retained RFP; (o) overlay. The bar in the last frame represents 5 μm.

© 2008 The Authors

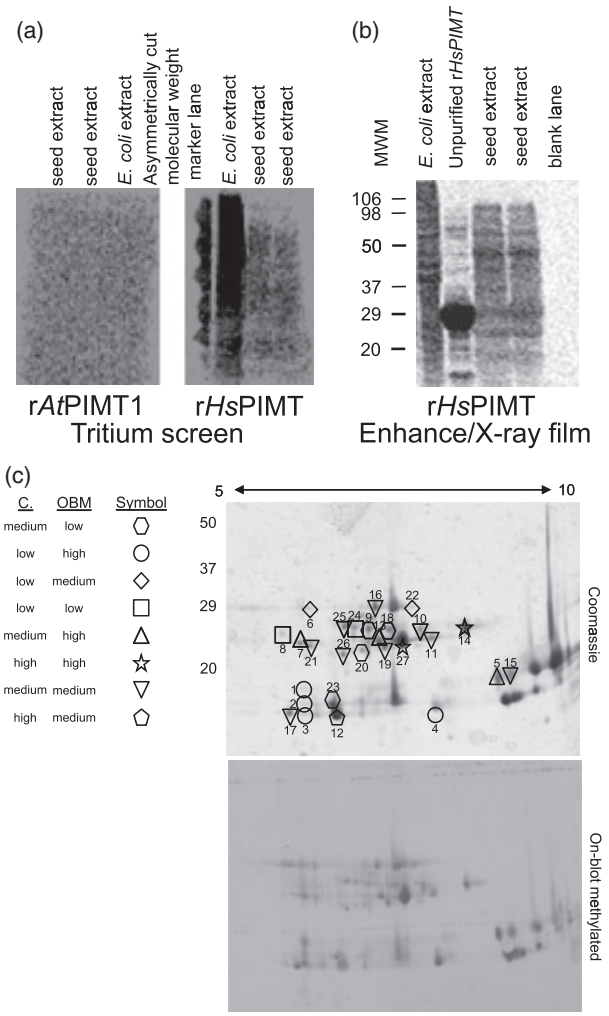

Figure 7. Arabidopsis seeds 6 h from completing germination have proteins and protein fragments containing isoaspartyl residues.
(a) Recombinant Arabidopsis PIMT1 or recombinant human PIMT was used to methylate blotted proteins from *Escherichia coli*, Arabidopsis seeds, and protein molecular weight markers. The blot was then visualized using a tritium screen.
(b) Resolution of on-blot-methylation (OBM) results improved using Enhance and X-ray film.
(c) A Coomassie stained two-dimensional gel of Arabidopsis seed proteins and an X-ray of proteins from a sister gel transferred to membrane and challenged with recombinant human protein-L-isoaspartate methyltransferase (PIMT) and tritiated *S*-adenosyl-L-methionine (AdoMet). The 27 proteins surrounded by a symbol on the stained gel were cored and their identities determined (see Table S2). The symbols in the legend and on the stained gel refers to the perceived abundance of the protein based on staining (C, Coomassie) and the relative intensity of the tritium signal from this protein after OBM.

high for many of the constructs, in spite of the fact that all the fusion constructs were expressed in the same context and driven by the CaMV 35S[2] promoter. We have previously documented that the TISI$\alpha\psi$ and TISI$\alpha\omega$ were specifically sequestered in the nucleus in onion epidermal cells (Xu *et al.*, 2004), where it is predicted to reside by both PSORT (Nakai and Horton, 1999) and TARGETP (Emanuelsson *et al.*, 2000; Table S1), albeit with low predicted confidence. In the present study, using tobacco epidermal cells, the PIMT2 TISI fusion proteins were present in the nucleus at low levels more akin to the lack of exclusion from, rather than active transport and sequestration in, this compartment. These conflicting results may reflect differences in monocot and dicot targeting machinery or may be due to the lack of chloroplasts *sensu stricto* in onion epidermal cells.

It appears that the N-terminal extension of the TISIII$\beta\psi$ isoform also targets the protein to the plastid. The PIMT TISIII was also observed to be associated with the ER as well as in specific consolidated spots. It may be that some of the targeting observed could be associated with stromules in chloroplast-to-chloroplast contact. However, some PIMT2 TISIII$\beta\psi$:GFP fluorescence was observed specifically in the ER.

The co-localization of PIMT2 TISIII$\alpha\psi/\alpha\omega$ (and possibly PIMT1) with AtMAP65 protein on tubulin was exciting. Tubulin is susceptible to isoaspartyl formation and is known to be a major endogenous PIMT substrate in both calf and rat brains (Aswad and Deight, 1983; Ohta *et al.*, 1987). The coexistence of the two proteins in high concentrations has been documented previously in brain and testis tissue, cell types having the highest PIMT-specific activities and high tubulin concentrations (Bouchard *et al.*, 1980; Diliberto and Axelrod, 1976). Najbauer *et al.* (1996) reported that both α- and β-tubulin have at least two sites susceptible to isoaspartate formation, that tubulin constantly undergoes isoaspartyl formation and, when PIMT is inhibited, accumulates these residues quickly. They conclude that for isoaspartyl to remain present at a low level in tubulin, as is the case *in vivo*, it must be continuously repaired by PIMT (Najbauer *et al.*, 1996).

Higher plants appear to be unique among eukaryotes in possessing two genes encoding PIMT (O'Connor, 2006; Xu *et al.*, 2004). In Arabidopsis, the *PIMT* variants produce recombinant proteins possessing PIMT activity *in vitro* (Thapar and Clarke, 2000; Xu *et al.*, 2004; Villa *et al.*, 2006; this report; data not shown). We have shown here that a complex *PIMT2* transcriptional and splicing regime exists that permits a catalytically competent PIMT2 to be deployed throughout the cell. Why is this not the case in other eukaryotes studied to date? One reason may be that plants producing orthodox seeds (those capable of surviving dehydration) require additional repair capacity for their proteome which, in the dehydrated state, is subjected to extended periods of stress and ionic insult (Brennan and Clarke, 1993; Hoekstra *et al.*, 2001; Ingrosso *et al.*, 1997). Exposure to stress increases isoaspartyl formation (and manifestation of the consequences) in many species (Kagan *et al.*, 1997; Kim *et al.*, 1997, 1999; Li and Clarke, 1992; Visick *et al.*, 1998). Indeed, for most plant species the preponder-

© 2008 The Authors

ance of PIMT activity has been recovered from seeds (Mudgett and Clarke, 1993, 1994; Mudgett *et al.*, 1997). Remarkably stable PIMT activity has been associated with seed viability in sacred lotus (*Nelumbo nucifera*) seeds several hundred years old (Shen-Miller *et al.*, 1995), while increases in isoaspartyl-containing proteins are associated with decreased seed viability (Kester *et al.*, 1997; Mudgett *et al.*, 1997).

The cruciferin storage proteins represent a special case where, destined for degradation and susceptible to alteration during development and germination (Job *et al.*, 2005), they acquire isoaspartate. Apparently it is more parsimonious for Arabidopsis to degrade these storage reserves as they are rather than expending AdoMet on their repair prior to digestion, Arabidopsis being equipped with an asparaginase capable of hydrolyzing isoaspartyl-containing peptide fragments (Bruneau *et al.*, 2006).

Arabidopsis microarray data of developmental stages (Schmid *et al.*, 2005) revealed that *PIMT2* transcription increased several-fold during seed development, whereas that of *PIMT1* remained fairly constant, corresponding well with independent semi-quantitative RT-PCR results (Xu *et al.*, 2004). Upon imbibition, *PIMT1* transcripts remain while those for *PIMT2* decline (Xu *et al.*, 2004). The amalgam of *PIMT2* transcripts was positively associated with the maintenance of seed dormancy in the extremely dormant Cape Verde Island ecotype of Arabidopsis, rapidly declining whenever seeds became capable of completing germination (Cadman *et al.*, 2006). This is a reasonable sequence of events if PIMT2 is responsible for the maintenance of the proteome extant in imbibed, dormant seeds where the energy (Gallardo *et al.*, 2002; Russell *et al.*, 2000) and machinery (Cadman *et al.*, 2006) required for *de novo* protein synthesis is deficient. Upon alleviation of dormancy, access to stored reserves conducive to protein synthesis is acquired (Kobrehel *et al.*, 1992; Lozano *et al.*, 1996; Yano *et al.*, 2001) and the importance of maintenance of the proteome relative to *de novo* synthesis may decline. A similar scenario exists in *Escherichia coli* lacking the *PIMT* gene. While the cells are in log phase, actively synthesizing protein, there are no obvious consequences of a lack of PIMT activity but, upon entering stationary phase where protein synthesis is limited, they are decimated (Li and Clarke, 1992). Studies of single and double *pimt* mutants in Arabidopsis are ongoing to determine whether there is a similar loss of vigor and/or viability associated with a decline in PIMT activity.

Experimental procedures

Plant material

Arabidopsis [*Arabidopsis thaliana* (L.) Heynh., ecotype Wassilewskija; Ws] seeds were moist chilled on germination blotter (Grade 628, Stults Scientific Engineering, http://www.stultsscientific.com/) in a Petri dish (Fisher Scientific, http://www.fishersci.com/) at 4°C for 3 days then transferred to 25°C under continuous fluorescent light (135 μmol m^{-2} sec^{-1}). Six hours prior to the completion of germination or 7 days after transfer to 25°C, seeds/seedlings were harvested for protein/RNA isolation, respectively. Alternatively, seedlings were transferred to soil and grown at 25°C with 16 h of fluorescent light daily (200 μmol m^{-2} sec^{-1}). Three weeks after transfer, plants were harvested, the soil removed from the roots, and RNA isolated from leaves and roots.

Tobacco seedlings (cv. KY160), the leaves from which were used for transient expression experiments, were grown aseptically on a minimal MS salts (Murashige and Skoog, 1962), 3%(w/v) sucrose, 0.8%(w/v) phytagar, 16/8 h light/dark cycles at 25°C. For bombardment, leaves were collected from 3 to 4-week-old seedlings.

Total RNA isolation from plant material.

Total RNA was isolated from rosette leaves using a kit (RNeasy Plant Kit, Qiagen Inc., http://www.qiagen.com/) and from seedlings using TRIZOL reagent (Invitrogen) according to the respective manufacturers' instructions. Total RNA was isolated from mature, dehydrated seeds using a hot borate technique (Wan and Wilkins, 1994).

5′-Rapid amplification of cDNA ends

Total RNA isolated from Arabidopsis rosette leaves was pretreated with DNaseI (DNA-*free*, Ambion Inc., http://www.ambion.com/) according to the manufacturer's instructions. The 5′-RACE procedures designed to amplify only capped mRNA were performed on 2.5 μg of DNaseI-treated leaf total RNA using gene-specific primers and a kit (GeneRacer, Invitrogen) according to the manufacturer's instructions.

The PCR was performed on 3 μl of first-strand cDNA, using gene-specific primers in conjunction with primers designed to the reverse transcribed RNA-adaptor ligated to the 5′-end of full length RNA in 5′-RACE (Invitrogen). Amplicons were isolated from 1%(w/v) agarose gels following electrophoresis, cloned into a T/A vector, and sequenced.

In separate experiments, a PCR primer identical to the cDNA sequence representing transcripts produced from the first transcriptional initiation site (*TIS I*; primer CH5F; Figure 1b) of the *PIMT2 TISI* was used with a reverse primer (CH5R; Figure 1b) binding to the second exon of all cDNAs to verify the presence of three splicing variants ($\beta\psi$, $\alpha\psi$, and $\alpha\omega$). The PCR reaction was run on a 4%(w/v) Metaphor agarose gel (Cambrex Inc., http://www.cambrex.com/) and then stained with 10 μg μl^{-1} SYBR Gold dye (Molecular Probes, http://www.probes.com/).

Primer extension assay

Primer extension assays were performed to map the transcription start sites as described in Triezenberg (1992) with slight modification. The first 21 nucleotides 5′ of the alpha splice site in the first intron (arrow with asterisk in Figure 1b) was used as a primer, 5′-end labeled with [γ^{32}P]ATP (3000 Ci $mmol^{-1}$, Perkin-Elmer Life and Analytical Sciences, Inc., http://www.perkinelmer.com/) using Optikinase (United States Biochemical (USB), Corporation, http://www.usbweb.com/) and column purified (ProbeQuant G-50 micro column; Amersham Pharmacia Biotech, http://www5.amersham biosciences.com/). Total RNA (50 μg) was hybridized with the 5′-end labeled oligonucleotide at 65°C for 90 min in 1.5 M KCl, 0.1 M

© 2008 The Authors

2-amino-2-(hydroxymethyl)-1,3-propanediol (TRIS)-Cl (pH 8.3) and 10 mM EDTA. The reaction was precipitated, washed, redissolved, and the primer allowed to extend with Superscript™ III RNase H⁻ Reverse Transcriptase (Invitrogen) at 50°C for 60 min. The product was RNase treated in the presence of salmon sperm DNA (100 μg ml^{-1}), precipitated, reconstituted, and resolved in 8% denaturing polyacrylamide gel containing 8.3 M urea. Sequencing reactions were performed in the presence of [α^{33}P] dATP with the same oligonucleotide on the *PIMT2 TISI-pNCO1T* plasmid using Sequenase Version 2.0 DNA Sequencing Kit (USB) and was resolved in the same gel as a sequencing ladder. The controls were PCR amplified from *PIMT2 TISI-pNCO1T* with the forward primer commencing from the longest 5′-RACE-predicted start sites of *PIMT2-TISI, TISII* and *TISIII* (Figure 1b) and the same end-labeled reverse primer used in the primer extension reaction. Once the TIS and splicing regimes were clarified, predicted protein sequences were analyzed using PredictProtein (http://www.predictprotein.org/; Rost, 1996) algorithms.

Recombinant protein production, purification, and enzyme assay:

Some splicing variants were cloned in frame into the *Xma*I, *Xho*I sites of pET43.1 (Novagen Inc., http://www.novagen.com) by introducing *Bsp*EI, *Sal*I 1 sites into the *PIMT2* 5′- and 3′-termini, respectively. The *PIMT2 TISIIIαψ* and αω and *PIMT2 TISIIαψ* coding regions were cloned into the *Nco*I, *Xho*I sites of pET23d (Novagen Inc.) using amplicon-introduced *Bsp*HI and *Sal*I sites. Recombinant human PIMT, the kind gift of Dr Steven Clarke (UCLA, USA) was subcloned into pET30b in-frame with a carboxy-terminal hexahistidyl tag. Recombinant protein production was induced in *E. coli* [BL21(DE3)RIL; Stratagene, http://www.stratagene.com/] and SDS-PAGE was used to determine solubility. All had some discernible protein in the soluble fraction except *PIMT2 TISIIαψ* which was purified as an inclusion body, solubilized in 6 M urea, diluted and tested for PIMT activity in 0.3 M urea. All other recombinant proteins were purified using nickel columns (Hi-Trap, GE Healthcare, http://www.gehealthcare.com/) and fast protein liquid chromatography (FPLC), and tested for activity (Mudgett and Clarke, 1993).

Antibody production and use

Antibodies were affinity-purified using recombinant protein from bacteria expressing PIMT1, PIMT2 TISIαω, PIMT2 TISIIαω, or PIMT2 TISIIIαω. Seven hundred and fifty micrograms of each recombinant protein was run in preparative 12% SDS-PAGE mini-gels and blotted to polyvinylidene fluoride (PVDF) membrane (Millipore Immobilon-P, http://www.millipore.com/). Blots were stained with Ponceau-S for visualization according to the instructions provided with the membrane and cut in 7.5 × 0.5 cm strips which were destained after excision.

One strip for each recombinant protein (PIMT1, PIMT2 TISI, TISII, and TISIII) was put in a tube and incubated (for 1 h) with 9 ml blocking solution [PBS, 0.02%(v/v) Tween-20, 1%(w/v) non-fat dry milk], slowly shaking at room temperature. One milliliter of serum containing antibody to PIMT2 that also cross-reacted with PIMT1 was added and incubation was continued for 1 h. The solution was discarded; the strips rinsed and washed for 3 × 5 min in PBS and transferred to a small glass culture tube. Bound antibody was eluted (4 ml 10 mM KH_2PO_4, pH 2.3) the culture tube capped, shaken vigorously, and poured into 6 ml ice-cold 50 mM K_2HPO_4 (bringing the pH to 7.0). The strips were rinsed (2 × 4.5 ml of water) and this wash combined with the first elution. The purified antibody was amended [80 mM NaCl, 3%(w/v) non-fat dried milk, 0.15%(v/v) Tween-20] adjusted to 25 ml and the preparation stored (4°C) until use. The PIMT2 TISI-specific antibody (Figure 3a; Xu *et al.*, 2004) was made by subsequently exposing the antibody, purified as above, to strips containing PIMT1 and retrieving the supernatant.

A crude nuclear preparation used 2 g wild-type Arabidopsis (WS) seeds ground in 10 ml isolation solution (50 mM potassium phosphate, pH 6.8, 10 mM NaCl, 300 mM sucrose). The paste was scraped into a beaker on ice with 50 ml isolation solution and stirred for 10 min. The sample volume was adjusted to 200 ml with isolation solution and filtered through two layers of cheesecloth and one layer of Miracloth, (Calbiochem, http://www.calbiochem.com). A pellet was obtained by centrifuging for 30 min at 2000 ***g*** at 4°C. This was washed twice by resuspending first in 50 ml and then in 15 ml of ice-cold isolation solution, and centrifuging for 15 min at 4000 ***g*** at 4°C. The final pellet was resuspended in 1 ml ice-cold isolation solution. A 1:100 dilution of the sample typically produced an OD_{595} of 0.35–0.5 (roughly 3–4.25 μg protein μl^{-1}) and 40 μg protein/well was resolved through 1.5 mm-thick SDS-PAGE mini-gels.

Western blots on PVDF membranes were blocked for 2 × 10 min [PBS, 3%(w/v) non-fat dried milk, 0.15%(v/v) Tween-20] with constant agitation and incubated in affinity-purified antibody (25 ml $blot^{-1}$) for 2 h at 23°C with agitation. Blots were rinsed in water and washed (PBS, 3 × 5 min) before incubation (2 h) in anti-rabbit IgG-horseradish peroxidase (HRP) conjugate (1:10,000; Sigma-Aldrich Co., http://www.sigmaaldrich.com/) in blocking solution. Blots were rinsed, washed (3 × 5 min in PBS), and developed according to the manufacturer's instructions (Amersham ECL) using Classic BX X-ray film (Molecular Technologies, http://www.moltec.net).

Transient expression of PIMT:GFP fusions

The *PIMT2* coding sequences were cloned downstream from the cauliflower mosaic virus $35S^2$ promoter in-frame with a 3′-situated GFP reporter in the binary vector, pKYLX80 (Dinkins *et al.*, 2003a; Schardl *et al.*, 1987). For positive controls in co-localization experiments DsRED or RFP (GenBank accession number DQ005474) were substituted for GFP in the pKYLX80 vector. Nuclear targeting used a portion of a zinc-finger protein in-frame with DsRED (Dinkins *et al.*, 2003b). For mitochondrial targeting, 180 bp of the 5′-coding sequence of the *A. thaliana ALTERNATIVE NAD(P)H DEHYDROGENASE* gene (*NDA2*; *At2g29990*; Michalecka *et al.*, 2003) was cloned in-frame with the *RFP* cDNA into the *Xho*I/*Sac*I sites of pKYLX80 RFP vector. For microtubule targeting, the full length *A. thaliana MICROTUBULE-ASSOCIATED PROTEIN 65-1* (*AtMAP65-1*; *At5g55230*), coding sequence was cloned into the *Bgl*II/*Sal*I sites of the pGD DsRED vector (Goodin *et al.*, 2002). For ER targeting, the pSITE:RFP vector (Chakrabarty *et al.*, 2007), containing ER targeting and retention sequences (GenBank accession number U87974; Haseloff *et al.*, 1997), were obtained from M. Goodin and R. Chakrabarty, University of Kentucky, Lexington, KY, USA.

Transient GFP/DsRED/RFP assays were conducted by introducing 100 ng DNA (per plasmid) (coated onto 1-μm diameter gold microcarriers; Bio-Rad Laboratories, http://www.bio-rad.com/) into tobacco leaf disk cells using a PDS1000 DuPont Bio-Rad Microprojectile delivery system (Bio-Rad Laboratories). Tobacco leaf disks were cultured for 24–48 h on media (Scott *et al.*, 1999). Disks were mounted on slides, and viewed in water under a coverslip using an Olympus FV1000 laser-scanning confocal microscope (Olympus America, Inc., http://www.olympusamerica.com/).

© 2008 The Authors

On-blot methylation

Two identical 1D and 2D gel electrophoreses of seed proteins were simultaneously prepared. One gel was stained with Coomassie Brilliant Blue while the other was transferred overnight to PVDF. After transfer, the PVDF membrane was blocked at 23°C [30 min in 0.2 mg ml^{-1} BSA, 10 mM 2-(*N*-morpholino)ethanesulfonic acid (MES), pH 6.2]. The proteins were subjected to OBM (Zhu *et al.*, 2006) at 23°C for 20 min in 500 μl [100 mM MES pH 6.2, 4 μM rHsPIMT, [^{3}H] AdoMet (10 μCi made to 10 μM in the reaction mix with cold AdoMet), 0.1 mg ml^{-1} BSA]. The blot was then rinsed briefly with water followed by washing with stop buffer (2 × 15 min in 10 mM MES pH 6.2, 50 μM *S*-adenosylhomocysteine (AdoHcy), 0.3 M NaCl, 0.05% v/v Tween 20). Finally, the blot was soaked in water for 5 min, sprayed with En3hance (PerkinElmer Life And Analytical Sciences, Inc.), dried, and exposed to X-ray film for 20 22 h. The developed film was placed under the Coomassie stained sister gel on a light box, and proteins cored from it.

Protein preparation and MALDI-TOF-TOF

Gel cores were minced, destained [2 × 0.5 h washes with 50 mM NH_4HCO_3/50% (v/v) CH_3CN followed by 10 min vortexing], dried in a vacuum centrifuge, and reduced by incubation at 57°C for 30 min (50 mM NH_4HCO_3, 10 mM DTT). The liquid was discarded and the proteins were alkylated (50 mM NH_4HCO_3, 50 mM iodoacetamide, incubated in the dark for 30 min at 23°C). The gel was washed (2 × 50 mM NH_4HCO_3; 1 × 100% CH_3CN) and partially dried in a vacuum centrifuge before being rehydrated [50 mM NH_4HCO_3, 10 ng μl^{-1} sequencing grade modified trypsin (Promega, http://www.promega.com/)] on ice for 1 h. An additional 50 mM NH_4HCO_3 was added to cover the sample and the gel was incubated for 18 h at 37°C.

Peptides were extracted from the gel, desalted, and concentrated by solid-phase extraction using a homemade device [0.1–10 μl pipette tip (no. 70.113, Sarstedt, http://www.sarstedt.com/)] packed with about 1 mm of Empore C-18 (no. 2215, 3M, http://www.3m.com/), and peptides were eluted in 3 μl of 50% (v/v) CH_3CN, 0.1% (v/v) trifluoroacetic acid (TFA). Desalted peptide extracts were spotted onto an Opti-TOF 384-well insert (Applied Biosystems/MDS Sciex, http://www.appliedbiosystems.com/) with 0.2 μl 5 mg ml^{-1} alpha-cyano-4-hydroxycinnamic acid (Sigma-Aldrich) in 50% (v/v) CH_3CN, 50% (v/v) 0.1% (v/v) TFA and made to 10 mM in $NH_4H_2PO_4$. Crystallized samples were washed with cold 0.1% (v/v) TFA and were analyzed by an Applied Biosystems 4800 MALDI-TOF-TOF Proteomics Analyzer. An initial MALDI MS spectrum was acquired for each spot (400 laser shots per spectrum) and a maximum of five peaks with a signal-to-noise ratio of >20 were automatically selected for tandem mass spectroscopy (MS/MS) analysis (1000 shots per spectrum) by post-source decay. Peak lists from the MS/MS spectra were submitted for database similarity searching using an in-house copy of MASCOT, Version 2.1 (Matrix Science, Inc., http://www.matrixscience.com/). The mass tolerance was ±0.5 Da for MS/MS precursor ions and ±0.1 Da for MS/MS product ions. Searches were against the NCBInr (10 November 2006, http://www.ncbi.nlm.nih.gov) database.

Acknowledgements

The authors are indebted to Dr Lynnette Dirk who assisted greatly with purification of the recombinant PIMT2 proteins. Dr Lisa Meeks provided the Arabidopsis MAP65 DNA, Dr Michael Goodin and Dr Romit Chakrabarty, the ER-targeted and retained RFP in the pSITE vector. Dr Steven Clarke kindly provided the human recombinant PIMT, and he and Dr Sarah Villa carefully scrutinized earlier drafts of the manuscript and provided many valuable suggestions for its improvement as did two anonymous referees. Research support was from a UK Department of Horticulture Stipend to QX, a DOE grant (no. DE-FG02-92ER20075) to RLH, and a NSF grant to ABD (MCB-0449646). The mass spectrometric analysis was performed at the University of Kentucky, Center for Structural Biology Protein Core Facility. This core facility is supported in part by funds from NIH National Center for Research Resources (NCRR) grant P20 RR020171.

Supplementary Material

The following supplementary material is available for this article online:

Figure S1. *Arabidopsis thaliana* (*At*)PIMT2 TIS I βΨ is targeted to the mitochondria.

Figure S2. *At*PIMT2 TIS II βΨ is imported into both mitochondria and chloroplasts.

Figure S3. Some *At*PIMT2 TIS IIIαω co-localizes with TUBULIN.

Figure S4. *At*PIMT2 TIS III βΨ appears to be located in the endoplasmic reticulum.

Table S1. Predicted protein localization for each PIMT2 protein based on two different algorithms.

Table S2. Identity of proteins and protein fragments from germinating Arabidopsis seeds approximately 6 h prior to the completion of this process that act as methyl acceptors for r*Hs*PIMT.

This material is available as part of the online article from http://www.blackwell-synergy.com.

Please note: Blackwell publishing are not responsible for the content or functionality of any supplementary materials supplied by the authors. Any queries (other than missing material) should be directed to the corresponding author for the article.

References

Aswad, D.W. and Deight, E.A. (1983) Purification and characterization of two distinct isozymes of protein carboxymethylase from bovine brain. *J. Neurochem.* **41**, 1702–1709.

Aswad, D.W., Paranandi, M.V. and Schurter, B.T. (2000) Isoaspartate in peptides and proteins: formation, significance, and analysis. *J. Pharm. Biomed. Anal.* **21**, 1129–1136.

Bouchard, P., Gagnon, C., Phillips, D.M. and Bardin, C.W. (1980) The localization of protein carboxyl-methylase in sperm tails. *J. Cell Biol.* **86**, 417–423.

Brennan, T.V. and Clarke, S. (1993) Spontaneous degradation of polypeptides at aspartyl and asparaginyl residues: effects of the solvent dielectric. *Protein Sci.* **2**, 331–338.

Bruneau, L., Chapman, R. and Marsolais, F. (2006) Co-occurrence of both L-asparaginase subtypes in *Arabidopsis*: At3g16150 encodes a K^+-dependent L-asparaginase. *Planta*, **224**, 668–679.

Cadman, C.S.C., Toorop, P.E., Hilhorst, H.W.M. and Finch-Savage, W.E. (2006) Gene expression profiles of Arabidopsis Cvi seeds during dormancy cycling indicate a common underlying dormancy control mechanism. *Plant J.* **46**, 805–822.

Chakrabarty, C., Banerjee, R., Chung, S.-M., Farman, M., Citovsky, V., Hogenhout, S.A., Tzfira, T. and Goodin, M. (2007) pSITE vectors for stable integration or transient expression of autofluorescent protein fusions in plants: probing *Nicotiana benthamiana*-virus interactions. *Mol. Plant Plant-Micobe Interact.* **20**, 740–750.

Clarke, S. (2003) Aging as war between chemical and biochemical processes: protein methylation and the recognition of age-damaged proteins for repair. *Ageing Res. Rev.* **2**, 263–285.

© 2008 The Authors

Curnis, F., Longhi, R., Crippa, L., Cattaneo, A., Dondossola, E., Bachi, A. and Corti, A. (2006) Spontaneous formation of L-isoaspartate and gain of function in fibronectin. *J. Biol. Chem.* **281**, 36466–36476.

David, C.L., Keener, J. and Aswad, D.W. (1999) Isoaspartate in ribosomal protein S11 of *Escherichia coli*. *J. Bacteriol.* **181**, 2872–2877.

Diliberto, E.J., Jr and Axelrod, J. (1976) Regional and subcellular distribution of protein carboxymethylase in brain and other tissues. *J. Neurochem.* **26**, 1159–1165.

Dinkins, R.D., Conn, H.M., Dirk, L.M.A., Williams, M.A. and Houtz, R.L. (2003a) The *Arabidopsis thaliana* PEPTIDE DEFORMYLASE 1 protein is localized to both mitochondria and chloroplasts. *Plant Sci.* **165**, 751–758.

Dinkins, R.D., Pflipsen, C. and Collins, G.B. (2003b) Expression and deletion analysis of an *Arabidopsis SUPERMAN*-like zinc finger gene. *Plant Sci.* **165**, 33–41.

Emanuelsson, O., Nielsen, H., Brunak, S. and von Heijne, G. (2000) Predicting subcellular localization of proteins based on their N-terminal amino acid sequence. *J. Mol. Biol.* **300**, 1005–1016.

Gallardo, K., Job, C., Groot, S.P.C., Puype, M., Demol, H., Vandekerckhove, J. and Job, D. (2002) Proteomics of Arabidopsis seed germination. A comparative study of wild-type and gibberellin-deficient seeds. *Plant Physiol.* **129**, 823–837.

Goodin, M.M., Dietzgen, R.G., Schichnes, D., Ruzin, S. and Jackson, A.O. (2002) pGD vectors: versatile tools for the expression of green and red fluorescent protein fusions in agroinfiltrated plant leaves. *Plant J.* **31**, 375–383.

Haseloff, J., Siemering, K.R., Prasher, D. and Hodge, S. (1997) Removal of a cryptic intron and subcellular localisation of green fluorescent protein are required to mark transgenic Arabidopsis plants brightly. *Proc. Natl Acad. Sci. USA*, **94**, 2122–2127.

Hoekstra, F.A., Golovina, E.A. and Buitink, J. (2001) Mechanisms of plant desiccation tolerance. *Trends Plant Sci.* **6**, 431–437.

Hoshi, T. and Heinemann, S. (2001) Regulation of cell function by methionine oxidation and reduction. *J. Physiol.* **531**, 1–11.

Ingrosso, D., Perna, A.F., D'Angelo, S., Buro, M.D., Malanga, P., Galletti, P., DeRosa, M. and Zappia, V. (1997) Enzymatic detection of L-isoaspartyl residues in food proteins and the protective properties of trehalose. *Nutr. Biochem.* **8**, 535–540.

Job, C., Rajjou, L., Lovigny, Y., Belghazi, M. and Job, D. (2005) Patterns of protein oxidation in Arabidopsis seeds and during germination. *Plant Physiol.* **138**, 790–802.

Kagan, R.M., Niewmierzycka, A. and Clarke, S. (1997) Targeted gene disruption of the *Caenorhabditis elegans* L-isoaspartyl protein repair methyltransferase impairs survival of dauer stage nematodes. *Arch. Biochem. Biophys.* **348**, 320–328.

Kester, S.T., Geneve, R.L. and Houtz, R.L. (1997) Priming and accelerated ageing affect L-isoaspartyl methyltransferase activity in tomato (*Lycopersicon esculentum* Mill.) seed. *J. Exp. Bot.* **48**, 943–949.

Kim, E., Lowenson, J.D., MacLaren, D.C., Clarke, S. and Young, S.G. (1997) Deficiency of a protein-repair enzyme results in the accumulation of altered proteins, retardation of growth, and fatal seizures in mice. *Proc. Natl Acad. Sci. USA*, **94**, 6132–6137.

Kim, E., Lowenson, J.D., Clarke, S. and Young, S.G. (1999) Phenotypic analysis of seizure-prone mice lacking L-isoaspartate (D-aspartate) *O*-methyltransferase. *J. Biol. Chem.* **274**, 20671–20678.

Kobrehel, K., Wong, J.H., Balogh, A., Kiss, F., Yee, B.C. and Buchanan, B.B. (1992) Specific reduction of wheat storage proteins by thioredoxin *h*. *Plant Physiol.* **99**, 919–924.

Li, C. and Clarke, S. (1992) A protein methyltransferase specific for altered Aspartyl residues is important in *Escherichia coli* stationary-phase survival and heat-shock resistance. *Proc. Natl Acad. Sci. USA*, **89**, 9885–9889.

Lindquist, J.A. and McFadden, P.N. (1994) Automethylation of protein (D-aspartyl/L-isoaspartyl) carboxyl methyltransferase, a response to enzyme aging. *J. Prot. Chem.*, **13**, 23–30.

Lowenson, J.D. and Clarke, S. (1991) Structural elements affecting the recognition of L-isoaspartyl residues by the L-isoaspartyl/D-aspartyl protein methyltransferase. Implications for the repair hypothesis. *J. Biol. Chem.* **266**, 19396–19406.

Lowenson, J.D. and Clarke, S. (1992) Recognition of D-aspartyl residues in polypeptides by the erythrocyte L-isoaspartyl/D-aspartyl protein methyltransferase. Implications for the repair process. *J. Biol. Chem.* **267**, 5985–5995.

Lozano, R.M., Wong, J.H., Yee, B.C., Peters, A., Kobrehel, K. and Buchanan, B.B. (1996) New evidence for a role for thioredoxin *h* in germinating and seedling development. *Planta*, **200**, 100–106.

Michalecka, A.M., Svensson, A.S., Johansson, F.I., Agius, S.C., Johanson, U., Brennicke, A., Binder, S. and Rasmusson, A.G. (2003) Arabidopsis genes encoding mitochondrial type II NAD(P)H dehydrogenases have different evolutionary origin and show distinct responses to light. *Plant Physiol.* **133**, 642–652.

Mudgett, M.B. and Clarke, S. (1993) Characterization of plant L-isoaspartyl methyltransferases that may be involved in seed survival: Purification, cloning and sequence analysis of the wheat germ enzyme. *Biochemistry*, **32**, 11100–11111.

Mudgett, M.B. and Clarke, S. (1994) Hormonal and environmental responsiveness of a developmentally regulated protein repair L-isoaspartyl methyltransferase in wheat. *J. Biol. Chem.* **269**, 25605–25612.

Mudgett, M.B., Lowenson, J.D. and Clarke, S. (1997) Protein repair L-isoaspartyl methyltransferase in plants' phylogenetic distribution and the accumulation of substrate proteins in aged Barley seeds. *Plant Physiol.* **115**, 1481–1489.

Murashige, T. and Skoog, F. (1962) A revised medium for rapid growth and bioassays with tobacco tissue cultures. *Physiol. Plant.* **15**, 473–497.

Najbauer, J., Orpisqewski, J. and Aswad, D.W. (1996) Molecular aging of tubulin: accumulation of isoaspartyl sites in vitro and in vivo. *Biochemistry* **35**, 5183–5190.

Nakai, K. and Horton, P.P. (1999) PSORT: a program for detecting the sorting signals of proteins and predicting their subcellular localization. *Trends Biochem. Sci.* **24**, 34–35.

O'Connor, C.M. (1987) Regulation and subcellular distribution of a protein methyltransferase and its damaged aspartyl substrate sites in developing *Xenopus* oocytes. *J. Biol. Chem.* **262**, 10398–10403.

O'Connor, C.M. (2006) Protein L-isoaspartyl, D-aspartyl *O-methyltransferases*: catalysts of protein repair. In *The Enzymes*, **Vol. XXIV** (Clarke, S.G. and Tamanoi, F., eds). Amsterdam, Boston, London: Elsevier Inc., pp. 385–433.

Ohta, K., Seo, N., Yoshida, T., Hiraga, K. and Tuboi, S. (1987) Tubulin and high molecular weight microtubule-associated proteins as endogenous substrates for protein carboxymethyltransferase in brain. *Biochimie*, **69**, 1227–1234.

Pliyev, B.K. and Gurvits, B.Y. (1999) Peptidyl-prolyl *cis-trans* isomerases: structure and functions. *Biochemistry (Mosc.)*, **64**, 738–751.

Reissnera, K.J. and Aswad, D.W. (2003) Deamidation and isoaspartate formation in proteins: unwanted alterations or surreptitious signals? *Cell. Mol. Life Sci.* **60**, 1281–1295.

Romero, H.M., Berlett, B.S., Jensen, P.J., Pell, E.J. and Tien, M. (2004) Investigations into the role of the plastidial peptide methionine sulfoxide reductase in response to oxidative stress in Arabidopsis. *Plant Physiol.* **136**, 3784–3794.

Rost, B. (1996) PHD: predicting one-dimensional protein structure by profile based neural networks. *Meth. Enzym.* **266**, 525–539.

© 2008 The Authors

Russell, L., Larner, V., Kurup, S., Bougourd, S. and Holdsworth, M.J. (2000) The Arabidopsis *COMATOSE* locus regulates germination potential. *Development*, **127**, 3759–3767.

Schardl, C.L., Byrd, A.D., Benzion, G., Altschuler, M.A., Hildebrand, D.F. and Hunt, A.G. (1987) Design and construction of a versatile system for the expression of foreign genes in plants. *Gene*, **61**, 1–12.

Schmid, M., Davison, T.S., Henz, S.R., Pape, U.J., Demar, M., Vingron, M., Scholkopf, B., Weigel, D. and Lohmann, J.U. (2005) A gene expression map of *Arabidopsis thaliana* development. *Nat. Genet.* **37**, 501–506.

Schumacher, R.J., Hansen, W.J., Freeman, B.C., Alnemri, E., Litwack, G. and Toft, D.O. (1996) Cooperative action of Hsp70, Hsp90, and DnaJ proteins in protein renaturation *Biochemistry*, **35**, 14889–14898.

Scott, A., Wyatt, S., Tsou, P.L., Roberston, D. and Strömgren, A.N. (1999) Model system for plant cell biology: GFP imaging in living onion epidermal cells. *Biotechniques*, **26**, 1125–1132.

Shen-Miller, J., Mudgett, M.B., Schopf, J.M., Clarke, S. and Berger, R. (1995) Exceptional seed longevity and robust growth: ancient sacred lotus from China. *Am. J. Bot.* **82**, 1367–1380.

Smertenko, A.P., Chang, H.-Y., Wagner, V., Kaloriti, D., Fenyk, S., Sonobe, S., Lloyd, C., Hauser, M.-T. and Hussey, P.J. (2004) The Arabidopsis microtubule-associated protein AtMAP65-1 molecular analysis of its microtubule bundling activity. *Plant Cell*, **16**, 2035–2047.

Talcott, B. and Moore, M.S. (1999) Getting across the nuclear pore complex. *Trends Cell Biol.* **9**, 312–318.

Tarcsa, E., Szymanska, G., Leckner, S., O'Connor, C.M. and Goldberg, A.L. (2000) Ca^{2+}-free calmodulin and calmodulin damaged by *in vitro* aging are selectively degraded by 26S proteasomes without ubiquitination. *J. Biol. Chem.* **275**, 20295–20301.

Thapar, N. and Clarke, S. (2000) Expression, purification, and characterization of the protein repair L-isoaspartyl methyltransferase from *Arabidopsis thaliana*. *Protein Expr. Purif.* **20**, 237–251.

Triezenberg, S.J. (1992) Preparation and analysis of RNA. Primer Extension. Unit 4.8, In *Supplement 20: Current Protocols in Molecular Biology* (Ausubel, F.M., Brent, R., Kingston, R.E., Moore, D.D., Seidman, J.G., Smith, J.A. and Struhl, K., eds). Hoboken, NJ, USA: John Wiley & Sons, Inc, pp. 4.8.1–4.8.5.

Villa, S.T., Xu, Q., Downie, A.B. and Clarke, S.G. (2006) Arabidopsis protein repair L-isoaspartyl methyltransferases: predominant activities at lethal temperatures. *Physiol. Plant.* **128**, 581–592.

Visick, J.E., Cai, H. and Clarke, S. (1998) The L-isoaspartyl protein repair methyltransferase enhances survival of aging *Escherichia coli* subjected to secondary environmental stresses. *J. Bacteriol.* **180**, 2623–2629.

Wan, C.-Y. and Wilkins, T.A. (1994) A modified hot borate method significantly enhances the yield of high quality RNA from cotton (*Gossypium hirsutum* L.). *Anal. Biochem.* **223**, 7–12.

Xie, M. and Schowen, R.L. (1999) Secondary structure and protein deamidation. *J. Pharmaceu Sci.* **88**, 8–13.

Xu, Q., Belcastro, M.P., Villa, S.T., Dinkins, R.D., Clarke, S.G. and Downie, A.B. (2004) A second protein L-isoaspartyl methyltransferase gene in *Arabidopsis* produces two transcripts whose products are sequestered in the nucleus. *Plant Physiol.* **136**, 2652–2664.

Yamamoto, A., Takagi, H., Kitamura, D. *et al.* (1998) Deficiency in protein L-isoaspartyl methyltransferase results in a fatal progressive epilepsy. *J. Neurosci.* **18**, 2063–2074.

Yano, H., Wong, J.H., Cho, M.-J. and Buchanan, B.B. (2001) Redox changes accompanying the degradation of seed storage proteins in germinating rice. *Plant Cell Physiol.* **42**, 879–883.

Zhu, J.X., Doyle, H.A., Mamula, M.J. and Aswad, D.W. (2006) Protein repair in the brain, proteomic analysis of endogenous substrates for protein L-isoaspartyl methyltransferase in mouse brain. *J. Biol. Chem.* **281**, 33802–33813.

© 2008 The Authors